Studies of Hard X–ray Tails in Z Sources with HEXTE/RXTE

Flavio D'Amico*, William A. Heindl†, Richard E. Rothschild† and Duane E. Gruber†

*Center for Astrophysics and Space Sciences, University of California, San Diego, and
Instituto Nacional de Pesquisas Espaciais - INPE
Av. dos Astronautas 1758, 12227-010 S. J. dos Campos, Brazil
†Center for Astrophysics and Space Sciences, University of California, San Diego
9500 Gilman Dr., La Jolla, CA 92093-0424

Abstract. We report *RXTE* results of spectral analyses of three (Sco X-1, GX 349+2, and Cyg X-2) out of the 6 known Z sources. No hard X–ray tails were found for Cyg X-2 ($<8.4\times10^{-5}$ photons cm^{-2} s^{-1}, 50–100 keV, 3σ) and for GX 349+2 ($<7.9\times10^{-5}$ photons cm^{-2} s^{-1}, 50–100 keV, 3σ). For Sco X-1 a variable hard X–ray tail (with an average flux of 2.0×10^{-3} photons cm^{-2} s^{-1}, 50–100 keV) has already been reported. We compare our results to reported detections of a hard component in the spectrum of Cyg X-2 and GX 349+2. We argue that, taking into account all the results on detections of hard X–ray tails in Sco X-1 and GX 349+2, the appearance of such a component is correlated with the brightness of the thermal component.

INTRODUCTION

The class of Z sources comprises 6 LMXBs (Sco X-1, GX 349+2, GX 340+0, Cyg X-2, GX 5−1, and GX 17+2) in which the primary is a neutron star with a low magnetic field ($\sim10^{10}$ G) accreting at or near the Eddington limit [1]. They share similar timing properties and are among the most luminous known LMXBs. The designation Z source results from the shape described in a x–ray color × color diagram (CD), with the movement along the Z interpreted in terms of changes in the mass accretion rate ($\dot{M}$, see, e.g., [1]). Apart from Sco X-1 and Cyg X-2, the Z sources are all found near the Galactic mid-plane (i.e., $b = 0°$).

Hard X–ray spectra from both Z and low luminosity atoll sources have already been reported in the literature [2-8]. The production of the hard X–ray tails in atoll sources has been presented in the context of various thermal emission models [9] from which the accretion geometry can be inferred. The situation is less clear for the Z sources, where non–thermal mechanisms are invoked to explain the production of such a component, and little, or nothing, is known about the details of the accretion geometry.

We are currently analyzing all of the Z source observations in the public *RXTE* database which contain long pointings. The aim is to create an uniform database that will allow us to make direct hard X–ray spectra comparisons. From this we expect to better understand the behavior of any non–thermal emission in these sources. We report here the preliminary results of this work, with data from 3 (Sco X-1, GX 349+2, and

Cyg X-2) out of the 6 known Z sources.

DATA SELECTION AND ANALYSIS

We used data from HEXTE [10] to search for hard X–ray tails in the spectrum of Sco X-1, GX 349+2, and Cyg X-2 in the $\sim$20–220 keV interval and data from PCA [11] to determine the position of the source in the CD and to study the 2–20 keV spectrum. We selected, from the public *RXTE* database, those subsets of data in which $\gtrsim$ 5000 s of HEXTE total on–source time was available, in order to achieve good sensitivity at high energies. Table 1 shows the selected subsets for GX 349+2 and Cyg X-2. The list of selected observations of Sco X-1 is given in [7]. We used XSPEC to analyze the PCA source spectra, using published models for GX 349+2 (a blackbody plus a disk-blackbody and an iron line, see [12]) and Cyg X-2 (an absorbed cutoff power-law plus an iron line, see [13]). A complex multicomponent model (an absorbed blackbody plus a power-law, a Comptonization spectrum, and a Gaussian line) was used to heuristically fit the PCA Sco X-1 spectra. Low enewrgy (20–50 keV) HEXTE spectra were fitted by a simple thermal bremsstrahlung. The hard X-ray component (i.e. $E > 50$ keV), found only in Sco X-1, was modeled as a simple power-law (see [6] for a more detailed description of the instrument and procedure used for data analysis). We carefully verified our background subtraction procedures, specially for GX 349+2, which is located near the Galactic mid-plane, where the diffuse Galactic Plane background up to $E \sim$ 800 keV [14] is known to vary in latitude [15]. We took advantage of HEXTE aperture modulation to remove this contribution to the background since HEXTE Cluster A measured the background at the same latitude as the source. Source confusion is also a concern for GX 349+2 due to the presence of 4U 1700−37 (see, e.g., [16]) inside the field of view of one of the regions used by HEXTE Cluster B to measure background (the B^- region). This is easily solved using only the B^+ region to measure the background for HEXTE Cluster B. We found no evidence of source confusion/contamination for Cyg X-2 and Sco X-1.

RESULTS

Cygnus X-2 and GX 349+2 were easily detected by HEXTE up to 50 keV. Nevertheless, the detection level was *always* below 3σ in the 50–75 keV band. We show in Fig. 1 a typical spectrum for Cyg X-2 and GX 349+2 together with a detection and a non-detection of a hard X–ray tail in Sco X-1.

All sources show some degree of variability in the 20-50 keV range. From the results in [7], for Sco X-1, a factor of 2 was detected, while it was a factor of 5 for Cyg X-2 and 2 for GX 349+2. Among the three, Cyg X-2 is the least luminous in the 2–20 keV energy range, with an average luminosity of 0.4 $L_{\rm Edd}$ (using d and $M_{\rm ns}$ measurements in [17]), while Sco X-1 and GX 349+2 emit at or above Eddington levels, for $M_{\rm ns} = 1.4\,M_\odot$ (see [18] and [19] for measured distances to Sco X-1 and GX 349+2, respectively). We found no evidence of the presence of a hard X–ray tail in our database for

TABLE 1. Selected *RXTE* observations of GX 349+2 and Cyg X-2

OBSID	MJD	$\mathbf{T}_{obs}$*	$\mathbf{T}_{HEX}$†	$\mathbf{F}_{(2-20)}$**	$\mathbf{F}_{(20-50)}$‡	$\mathbf{F}_{(50-100)}$§	Z¶
GX 349+2							
20054-05-01-00	50570	10032	5902	$1.75^{+0.09}_{-0.09}$	$2.03^{+0.43}_{-0.41}$	< 4.64	SA
30042-02-01-01	50822	8688	5492	$2.42^{+0.22}_{-0.17}$	$3.94^{+0.59}_{-0.52}$	< 5.52	FB
30042-02-01-02	50823	10336	6527	$1.98^{+0.06}_{-0.06}$	$3.46^{+0.48}_{-0.48}$	< 6.28	(lower) NB
30042-02-01-07	50823	14160	8850	$1.95^{+0.02}_{-0.02}$	$2.87^{+0.34}_{-0.34}$	< 1.37	SA
30042-02-01-03	50825	13728	8602	$2.50^{+0.25}_{-0.22}$	$3.94^{+0.08}_{-0.83}$	< 4.84	FB
30042-02-01-04	50826	14304	8865	$2.55^{+0.20}_{-0.18}$	$2.56^{+0.28}_{-0.26}$	< 3.71	FB
30042-02-01-08	50826	10368	6318	$2.08^{+0.25}_{-0.25}$	$4.97^{+0.45}_{-0.45}$	< 3.17	FB
30042-02-02-00	50830	9760	5632	$1.72^{+0.07}_{-0.07}$	$2.46^{+0.44}_{-0.44}$	< 5.32	NB-FB
30042-02-02-08	50838	7704	4689	$1.71^{+0.08}_{-0.08}$	$2.10^{+0.48}_{-0.46}$	< 6.49	NB-FB
30042-02-03-01	50842	9216	5684	$2.71^{+0.49}_{-0.32}$	$4.22^{+0.51}_{-0.46}$	< 2.97	FB
Cyg X-2							
10063-10-01-00	50316	8088	5044	$1.16^{+0.35}_{-0.39}$	$8.37^{+4.77}_{-4.44}$	< 6.92	FB
30418-01-05-00	51000	10760	6349	$1.14^{+0.14}_{-0.18}$	$5.62^{+4.22}_{-3.82}$	< 4.12	FB
30046-01-01-00	51009	13376	8180	$1.88^{+0.13}_{-0.13}$	$21.89^{+3.50}_{-3.28}$	< 4.61	SA
30046-01-02-00	51015	14736	9240	$1.65^{+0.07}_{-0.15}$	$15.26^{+3.66}_{-3.66}$	< 4.21	FB
30046-01-03-00	51022	13728	8881	$1.42^{+0.30}_{-0.28}$	$28.03^{+3.64}_{-3.64}$	< 4.88	FB
30046-01-04-00	51029	13584	8157	$1.23^{+0.09}_{-0.10}$	$9.74^{+3.12}_{-3.02}$	< 1.78	FB
30046-01-06-00	51041	15104	9114	$1.76^{+0.18}_{-0.21}$	$15.56^{+3.11}_{-3.11}$	< 4.86	FB
30046-01-07-00	51048	13888	8231	$1.35^{+0.09}_{-0.11}$	$5.38^{+3.34}_{-3.12}$	< 3.02	FB
30046-01-08-00	51055	13920	8566	$1.20^{+0.06}_{-0.06}$	$25.95^{+3.37}_{-3.37}$	< 4.40	NB
30046-01-09-00	51061	16256	9010	$1.30^{+0.08}_{-0.08}$	$6.54^{+3.07}_{-2.88}$	< 3.62	FB
30046-01-10-00	51068	8600	5419	$1.81^{+0.11}_{-0.13}$	$23.97^{+5.03}_{-5.03}$	< 3.03	SA
30046-01-11-00	51078	12512	8098	$1.48^{+0.10}_{-0.12}$	$9.24^{+3.88}_{-3.60}$	< 3.96	FB
30046-01-12-00	51081	14608	9703	$1.37^{+0.01}_{-0.01}$	$29.16^{+3.50}_{-3.50}$	< 7.01	HB

* total *RXTE* source's exposure time, in s

† corrected HEXTE exposure time, in s

** Flux, in 2-20 keV range, in units of 10^{-8} ergs cm^{-2} s^{-1}; uncertainties are given at 90% confidence level

‡ Flux, in 20-50 keV range, in units of 10^{-10} ergs cm^{-2} s^{-1}, for GX 349+2, and 10^{-11} ergs cm^{-2} s^{-1}, for Cyg X-2; uncertainties are given at 90% confidence level

§ 3σ upper limit on power-law Flux, in units of 10^{-11} ergs cm^{-2} s^{-1}, in the 50-100 keV range; power-law index frozen at a value of 2

¶ HB=horizontal branch; NB=normal branch; FB=flaring branch; SA=soft apex

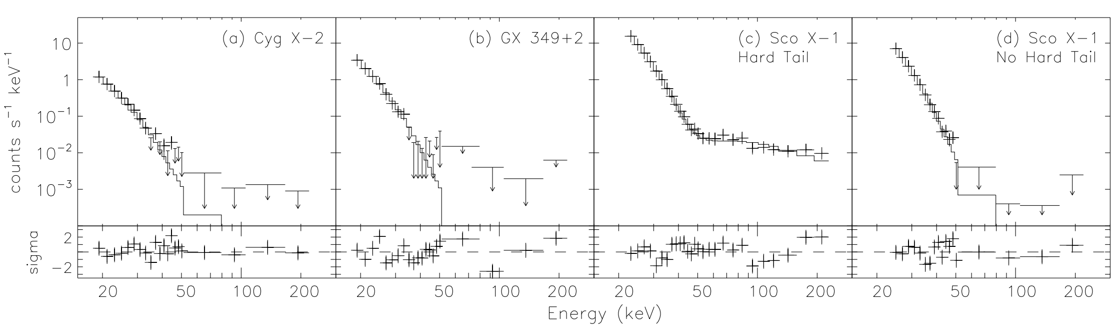

FIGURE 1. Typical HEXTE spectra (upper panels) for (a) Cyg X-2, (b) GX 349+2, (c) a hard X-ray tail detection in Sco X-1, and (d) a non-detection in Sco X-1 (for comparison). Residuals are given in units of standard deviations (lower panels). Upper limits are 2σ.

GX 349+2 or Cyg X-2. The HEXTE 3σ upper limit to 50–100 keV flux from GX 349+2 is 7.9×10^{-5} photons cm^{-2} s^{-1} and for Cyg X-2 is 8.4×10^{-5} photons cm^{-2} s^{-1}. For these two sources, a hard X–ray tail was, however, reported by *BeppoSAX* ([8] and [3], respectively), at a level of 4.6×10^{-4} photons cm^{-2} s^{-1} for GX 349+2 (using the fit parameters given in [8]; for Cyg X-2 it is not possible to estimate the flux from [3]). Our results, thus, can be interpreted in terms of variability in the appearance of this component, as was observed in Sco X-1 [7] on a 4 hour time-scale.

DISCUSSION

Scorpius X-1 remains as a special case among the Z sources. It is the only one in which a hard X–ray tail has been observed more than once, and by two different instruments ([5] and [7]). For Cyg X-2, GX 17+2 and GX 349+2 hard X–ray tails were reported by *BeppoSAX* ([3], [4], and [8], respectively) on one occasion. From our combined HEXTE database, we found the presence of a hard X–ray tail in 8 out of 28 occasions for Sco X-1, and zero out of 10 and 13 observations of GX 349+2 and Cyg X-2, respectively. Fitting our HEXTE data for GX 349+2 and Cyg X-2 with a power-law with indices frozen in the range 1–2 (within the values found for those three sources: see [3], [7-8]), we found a 3σ upper limit on the luminosity of the power-law component, $L^{\rm PL}_{\rm 20\text{-}80\,keV} = 6.8 \times 10^{35}$ ergs s^{-1} and $L^{\rm PL}_{\rm 20\text{-}80\,keV} = 5.0 \times 10^{35}$ ergs s^{-1} for GX 349+2 and Cyg X-2, respectively. Our HEXTE result (for $\Gamma = 1-2$) for hard X–ray tail detections in Sco X-1 is $L^{\rm PL}_{\rm 20\text{-}80\,keV} = 6.7 \times 10^{35}$ ergs s^{-1}. It thus appears that our observations were sensitive enough to detect hard X–ray tails in Cyg X-2 and GX 349+2. As we pointed out in [7] the chance of observing a hard X–ray tail (in Sco X-1) is higher when the thermal component of the spectrum is brighter. From our results here (see Table 1), we have, for GX 349+2 $L^{\rm Thermal}_{\rm 20\text{-}50\,keV}$ = 1.2–3.1 $\times 10^{36}$ergs s^{-1}, while for Cyg X-2 the results are $L^{\rm Thermal}_{\rm 20\text{-}50\,keV}$ = 0.4–2.1 $\times 10^{36}$ergs s^{-1}. The same component in Sco X-1, when a hard tail is detected [7], is in the range $L^{\rm Thermal}_{\rm 20\text{-}50\,keV}$ = 4.5–9.0 $\times 10^{36}$ergs s^{-1}. While comparable values were not given by the *BeppoSAX* results in [3], [4], and [8] (nor by the OSSE/*CGRO* results in [5]), it is possible to extrapolate the results presented in [8] in order to find an estimate of the luminosity of the thermal component. We estimate that the 20–50 keV GX 349+2 luminosity measured by *BeppoSAX* was greater than 5×10^{36} ergs s^{-1}. Thus, one can speculate that the production of a hard X–ray tail in a Z source is a process triggered when the thermal component is brighter than a level of $\sim 4 \times 10^{36}$ ergs s^{-1}.

CONCLUSIONS

We have shown *RXTE* results of broad-band spectral analyses of three Z sources, with emphasis on the hard X–ray spectrum. We found no evidence for a detection of a hard X–ray tail in the spectra of GX 349+2 and Cyg X-2, although one detection of such a component has been reported for each of these sources. We interpret this in terms of variability, which was shown to be as fast as 4 hours in Sco X-1. We found an indication that the production of hard X–ray tails in Z sources is a process triggered when the

thermal component brightness is above a value of $\sim 4 \times 10^{36}$ ergs s^{-1}. We are currently creating a uniform HEXTE database including the other three Z sources (GX 17+2, GX 340+0, and GX 5−1), from which we hope to be able to better understand the production of hard X–ray in Z sources.

ACKNOWLEDGMENTS

This research has made use of data obtained through the HEASARC, provided by NASA/GSFC. F.D. gratefully acknowledges FAPESP/Brazil for financial support under grant 99/02352-2. This research was supported by NASA contract NAS5-30720.

REFERENCES

1. van der Klis, M., *X-Ray Binaries*, edited by W. H. G. Lewin, J. van Paradjis, and E. P. J. van den Heuvel, Cambridge University Press, Cambridge, 1995, pp.252–307.
2. Barret, D. et al., *ApJ* **533**, 329-351 (2000).
3. Frontera, F. et al., *Nucl. Phys. B* **69**, 286-293 (1998).
4. Di Salvo, T. et al., *ApJ* **544**, L119-L122 (2000).
5. Strickman, M., and Barret, D. 2000, "Detections of Multiple Hard X-ray Flares from Sco X-1 with OSSE", in *Proceedings of the Fifth Compton Symposium*, edited by M. L. McConnel and J. M. Ryan, AIP Conference Proceedings 510, New York, 2000, pp. 222-226.
6. D'Amico, F. et al., *ApJ* **547**, L147-L150 (2001).
7. D'Amico, F. et al., *Adv. Spa. Res.*, in press (2001) (astro-ph/0101396).
8. Di Salvo, T. et al., *ApJ*, in press (2001) (astro-ph/0102299).
9. Barret, D., *Adv. Spa. Res.*, in press (2001) (astro-ph/0101295).
10. Rothschild, R. E. et al., *ApJ* **496**, 538-549 (1998).
11. Jahoda, K. et al., *Proc. SPIE* **2808**, 59-70 (1996).
12. Christian, D. J., and Swank, J. H., *ApJS* **109**, 177-224 (1997).
13. Kuulkers, E. et al., *A&A* **323**, L29-L32 (1997).
14. Boggs, S. E. et al., *ApJ* **544**, 320-329 (2000).
15. Valinia, A., and Marshall, F. M., *ApJ* **505**, 134-147 (1998).
16. Reynolds, A. P. et al., *A&A* **349**, 873-876 (1999).
17. Orosz, J., and Kuulkers, E., *MNRAS* **305**, 132-142 (1999).
18. Bradshaw, C. F., Fomalont, E. B., and Geldzahler, B. J., *ApJ* **512**, L11-L14 (1999).
19. McNamara, D. H. et al., *Pub. Astr. Soc. Pac.* **112**, 202-216 (2000).